Pergamon

Geochimica et Cosmochimica Acta, Vol. 66, No. 19, pp. 3367–3374, 2002

0016-7037/02 $22.00 + .00

PII S0016-7037(02)00949-3

Microbial respiration and diffusive transport of O_2, $^{16}O_2$, and $^{18}O^{16}O$ in unsaturated soils: A mesocosm experiment

M. Jim Hendry,[1] Leonard I. Wassenaar,[2,*] and Tyler K. Birkham[1]

[1]Department of Geological Sciences, 114 Science Pl., University of Saskatchewan, Saskatoon, SK S7N 52, Saskatchewan, Canada
[2]National Water Research Institute, Environment Canada, Saskatoon, S7N 3H5, Saskatchewan, Canada

(*Received December* 20, 2001; *accepted in revised form April* 12, 2002)

Abstract—Although the flux of molecular O_2 between the atmosphere and the subsurface is intrinsically linked to the net soil production of greenhouse gasses, few studies have focused on the controls affecting the isotopic composition of O_2 in the subsurface. Here, we developed and tested a stable oxygen isotope tracer technique and gas transport modeling approach to evaluate O_2 cycling and fluxes from the subsurface that used an environmentally controlled soil mescosm. We measured the O_2 and $\delta^{18}O_2$ profiles in a model unsaturated soil zone and quantified the O_2 consumption rates and the O_2 isotope fractionation factors resulting from the combined processes of subsurface microbial (including bacteria, fungi, and protozoa) consumption of O_2 and diffusive influx of O_2 from the atmosphere. We found that at high respiration rates in the mesocosm, there appeared to be very little isotope fractionation of O_2 by soil microorganisms. Although the mesocosm respiration rates are not typical of natural soils in northern temperate climes, they may be more representative of soils in warm and moist tropical environments. Our findings caution against the indiscriminate application of laboratory-determined oxygen isotope fractionation factors to field settings. The oxygen isotope tracer and modeling approach demonstrated here may be applied to gain a better understanding of biogenic gas production and O_2 cycling in subsurface systems and soils. *Copyright © 2002 Elsevier Science Ltd*

1. INTRODUCTION

An understanding of the nature of biogenic gas fluxes between the atmosphere, biosphere, hydrosphere, and the subsurface is critical to a clearer understanding of the causes of changes in atmospheric gas compositions and for improving model predictions of global climatic change. Over the past two decades, considerable attention has focused on radiatively important biogenic trace gases such as CO_2 and CH_4 (e.g., Blake and Rowland, 1988; Matson and Harris, 1995; Trumbore et al., 1996). However, it is also well established that nongreenhouse gases such as molecular O_2 also play a critical role the biogeochemistry of global carbon cycling. Molecular oxygen (O_2) availability, or lack thereof, plays a critical role in the activity and respiration of subsurface microorganisms, in the oxidation of soil and dissolved organic matter, and in numerous biogeochemical reactions that can occur in unsaturated zones. Because O_2 is a terminal electron acceptor and the most biochemically active oxidant (Stumm and Morgan, 1981), the presence or absence of O_2 in the subsurface will greatly impact the rate and extent of biodegradation of contaminants, the oxidation state of transitional metals (Langmuir, 1997), microbial respiration of biogenic CO_2, and the amount of dissolved oxygen recharging ground waters (Rose and Long, 1988; Neale et al., 2000). Rates of aerobic microbial degradation of organic matter and contaminants in the subsurface are greater than anaerobic degradation. Hence, an understanding of the physical transport mechanisms and the biogeochemical processes that control O_2 concentrations and fluxes to and within the subsurface are needed. To date, there has been comparatively little attention paid to the O_2 side of biogenic gas production and fluxes to and from the subsurface.

Microbial aerobic respiration and oxidation of organic matter are generally considered to be the primary sinks for O_2 and main sources of elevated biogenic CO_2 concentrations in the subsurface. Because atmospheric CO_2 concentrations are negligible (0.036 vol%), CO_2 measurements have frequently been employed as an easily measurable index of microbial respiration in unsaturated geologic media. As a result, estimates of subsurface microbial respiration and organic carbon biodegradation have primarily been obtained by measuring CO_2 gas production in microcosm experiments (cf. Chapelle, 1992; Hendry et al., 2001), by modeling CO_2 gas concentrations in vertical geologic depth profiles (cf. Wood and Petraitis, 1984; Solomon and Cerling, 1987; Wood et al., 1993; Revesz et al., 1995; Hendry et al., 1999), and by measuring CO_2 effluxes from soil surfaces (cf. Hall et al., 1990; Rochette et al., 1991; Norman et al., 1992; Striegl and Wickland, 1998; Kabwe et al., 2002).

Despite the obvious importance of O_2 to subsurface microbial respiration, biodegradation and biogenic gas production in the subsurface, only a few studies have used detailed depth profiles of O_2 gas concentrations to determine the rates of biogeochemical reactions or microbial activity in unsaturated zones (e.g., Wood and Petraitis, 1984). Furthermore, fewer studies still have used the stable isotopic composition and fractionation of the stable isotopes of O_2 ($^{18}O/^{16}O$) in unsaturated geologic media as a tracer of microbial degradation of contaminants (Aggarwal et al., 1997; Aggarwal and Dillon, 1998) and O_2 gas transport (Severinghaus et al., 1996). Although the source of O_2 in unsaturated geologic media is the atmosphere (O_2 = 20.9 vol%, $\delta^{18}O$ = +23.5‰, Vienna standard mean ocean water [VSMOW]), its concentration and

* Author to whom correspondence should be addressed (jim.hendry@usask.ca).

stable isotopic composition in the subsurface may subsequently be altered by microbial respiration and diffusive transport.

Respiration preferentially consumes ^{16}O, leaving the remaining molecular O_2 enriched in ^{18}O. This isotope enrichment of atmospheric oxygen (relative to ocean water) is known as the Dole effect (Lane and Dole, 1956; Bender et al., 1994) and is intrinsically linked to global oxygen and carbon cycling. Isotope fractionation during respiration may be negligible if O_2 is scarce. In this case, any O_2 isotope available is consumed. Oxygen scarcity may occur in root tissues or soil aggregates where there is an increased resistance to O_2 migration (Angert and Luz, 2001). Diffusive fractionation occurs when ^{16}O migrates more quickly than ^{18}O along a concentration gradient. This fractionation depletes ^{18}O relative to ^{16}O as O_2 concentrations decrease. Other potential oxygen consuming and isotope fractionating processes such as mineral oxidation (Taylor et al., 1984), gravitational settling (Severinghaus et al., 1996), and isotopic exchange with oxy-anions and water are generally considered to be negligible under most natural conditions (Aggarwal and Dillon, 1998).

Microbial respiration is the largest global processor of O_2 and has been shown to result in the significant and preferential consumption of the lighter isotope, resulting in isotopic enrichment of residual O_2 (Schleser, 1979; Hoefs, 1987) and concomitant production of biogenic CO_2. Reported oxygen isotopic fractionation factors (α_k) for microbial consumption of O_2 in lab and field tests range from 0.971 to 0.999 (Lane and Dole, 1956; Schleser, 1978, 1979; Guy et al., 1989, 1993; Bender, 1990; Kiddon et al., 1993; Aggarwal and Dillon, 1998; Revesz et al., 1999; Angert et al., 2001). Angert and Luz (2001) reported α_k values from 0.980 to 0.988 for root respiration. Typically, an α_k value of 0.982 is used as the respiration fractionation factor for studies involving the Dole effect (Bender et al., 1994). However, if O_2 is scarce, respiration processes will consume any O_2 available, and α_k will approach 1.000 (Angert and Luz, 2001).

In the specific case of gaseous O_2 flux into soil and the deeper subsurface by molecular diffusion, the preferential movement of the lighter isotope results in the enrichment of the lighter isotope (e.g., tendency toward lower δ values) with decreasing pore gas O_2 concentrations. According to Graham's Law (Clark and Fritz, 1997), the kinetic isotopic fractionation factor for molecular diffusion (α_D) of O_2 is 0.986. The actual $\delta^{18}O$ values of the subsurface O_2, however, depend on both diffusive and consumptive fractionation.

Clearly, the exchange of biogenic gases from the subsurface to the atmosphere depends on biotic and abiotic factors such as microbial respiration and physical gas transport properties at a variety of spatial scales. Here we develop a stable isotopic tracer and transport modeling approach to aid in evaluating O_2 cycling and fluxes from the subsurface by employing an environmentally controlled mesocosm model. We measured the O_2 and $\delta^{18}O$ profiles in a model unsaturated soil zone and quantified the O_2 consumption rates and the stable oxygen isotope fractionation factors resulting from the combined processes of subsurface microbial consumption of O_2 and diffusive influx of O_2 from the atmosphere. Detailed, one-dimensional, O_2 and $\delta^{18}O$ profiles were obtained from a large-scale model mesocosm, which was filled with unsaturated C-horizon sand. The mesocosm provided a tightly controlled environment for conducting detailed process-related research under steady-state conditions (Lawrence et al., 1993; Hendry et al., 2001), conditions that are normally nonexistent under variable and seasonal field conditions (Papendick and Runkles, 1965). Our results were also compared with a previous long-term study of biogenic soil CO_2 production and fluxes using the same mesocosm (Hendry et al., 1999). Whereas the isotope tracer and O_2 flux results from this highly controlled mesocosm study may not be directly transferable to more complex natural environments, the combined isotope tracer and gas transport modeling approach we have developed and tested here through the use of a controlled mesocosm can be applied to the study of biogenic gas fluxes and O_2 cycling in natural environments.

2. MATERIALS AND METHODS

2.1. Description of the Mesocosm

Fine-grained sand was excavated from the C-horizon of an unsaturated zone at a local field site located near Saskatoon, Saskatchewan, Canada (52.05 N, 106.36 W). The sand was excavated to a depth of 6 m with a 2-m-diameter solid-stem auger in November 1992. As it was excavated, the 65 tonnes of sand was placed on plastic sheets and immediately transported to the laboratory.

The bottom 0.5 m of a fiberglass mesocosm (2.4 m in diameter by 4.6 m high) was filled with 6- to 12-mm-diameter gravel to facilitate control of the water table. The sand excavated from the field site was placed on top of the gravel in the opposite order to which it was removed from the field site. The sand was emplaced under standing water and vibrated to minimize the amount of air entrapped during filling. This also increased the bulk density and floated out any root material out of the sand. Root material was continuously skimmed off the water surface during filling. The final bulk density and porosity in the sand was 1.52 $g \cdot cm^{-3}$ and 0.426 ($n = 9$). These values approximated those for the C-horizon at the field site (average bulk density of 1.51 $g \cdot cm^{-3}$ and porosity of 0.433; Hendry et al., 1999). It is important to note that the sand was relatively homogeneous and contained no organic soil horizons (i.e., no A- or B-horizons or roots). The volume of excavated material yielded a final sand thickness of 3.6 m in the mesocosm. The texture and geochemistry of the sand, method of excavation, mixing, filling, and instrumentation of the mesocosm are fully described elsewhere (Hendry et al., 2001).

After filling the mesocosm, the water table was lowered from ground surface to a depth of 3.2 m on December 28, 1992. The lowering of the water table was assigned day 1 of the experiment. A uniformly distributed volume of distilled water was applied to the surface of the mesocosm on a weekly basis (30 $L \cdot wk^{-1}$), with a rain simulator system used since then. Depth to water table, moisture content (measured with a neutron probe), water drainage flux, and temperature in the mesocosm (measured with thermocouples) were measured routinely. Steady-state conditions with respect to water content and drainage flux were reached after days 200 and 633, respectively (Hendry et al., 2001). To ensure that the system was at steady state with respect to both soil gas and soil moisture contents, the time period of interest to the current study was selected to be from day 2254 to day 2602. This time frame also corresponded to our ability to first conduct gaseous O_2 stable isotope tracer analyses (Wassenaar and Koehler, 1999).

2.2. Collection and Analysis of Gas Samples

Gas samples were collected from duplicate installed bundles of soil gas samplers. The gas samplers were constructed of stainless steel tubes (6.3 mm inner diameter) with 50-mm perforated tips and installed at depths of 0.22, 0.48, 0.98, 1.48, 2.00, and 2.53 $\pm$ 0.03 m below surface in the east bundle, and 0.20, 0.46, 0.96, 1.46, 1.98, and 2.51 $\pm$ 0.03 m below surface in the west bundle. The gas sampling bundles were located $\sim$2 m apart in the mesocosm. Gas samples were collected from the sampling ports with 60-mL plastic gas-tight syringes. Gas concentration (O_2 and CO_2) analyses were performed within 1 hr of sampling with a Carle Special Series Model 311 gas chromatograph (GC),

equipped with Porapak and molecular sieve packed columns with automatic valve switching. The GC was equipped with thermal conductivity and flame ionization detectors. Gas samples were collected and analyzed on a weekly to biweekly basis from day 1 to 840 and from day 2254 to 2602. No gas sampling and gas composition analyses were conducted between days 841 and 2253, although the mesocosm was maintained with routine irrigation. The results of CO_2 gas analyses from day 1 to 840 are presented and discussed in Hendry et al. (2001).

Gas samples for stable oxygen isotope analysis of O_2 were collected from the sampling ports with gas-tight syringes. Thirty milliliters of soil gas was initially purged from each gas sampling port to flush the probe and syringe before sample collection and eliminate potential atmospheric oxygen contamination. Gas samples (~1 mL) were collected in 5-mL syringes and taken directly to a stable isotope-ratio mass-spectrometer for analysis of $^{18}O/^{16}O$ of the soil gas oxygen. A three-way valve and needle (21 gauge) fitted on each sample gas syringe was positioned to enable flushing of the needle with He to eliminate atmospheric O_2. Although flushing the needle with He, the injection needle was capped with a septum and was ready for isotopic analysis. All O_2 samples were measured for $\delta^{18}O$ on a Micromass Optima by the method described by Wassenaar and Koehler (1999). Pure O_2 was used as the analysis gas (by complete gas chromatographic separation of O_2 and N_2), and as the isotopic reference gas. The $\delta^{18}O$ values of sample oxygen were calculated by measurement of O_2 isotopes at m/z 34/32 and comparison to a reference pulse of O_2. Atmospheric oxygen was assumed to have a $\delta^{18}O$ value of +23.5‰ with respect to VSMOW according to Kroopnick and Craig (1972), and air O_2 was used to correct soil gas and reference gas values. Sample reproducibility for $\delta^{18}O$ was better than ± 0.2‰.

2.3. Numerical Modeling of the O_2, $^{16}O_2$, and $^{18}O^{16}O$ Concentrations

A numerical model was used to simulate the microbial consumption of O_2, $^{16}O_2$, and $^{18}O^{16}O$, assuming steady-state diffusive transport of the gases in the unsaturated mesocosm. The numerical model was based on a solution developed to model transient gas transport and consumption/production in unsaturated media (Hendry et al., 1999). It used a finite-element method to solve the one-dimensional gas diffusion and consumption/production equations for steady-state conditions:

$$\theta_a D^* \frac{\partial^2 c}{\partial z^2} - \rho_b G^* = 0, \tag{1}$$

with initial and boundary conditions of

$$c(z, 0) = c_i,$$

$$c(0, t) = c_o, \text{ and}$$

$$\partial c/\partial z\,(L, t) = 0, \tag{2}$$

where c is the concentration of O_2 (vol%), c_o is the atmospheric concentration of O_2 (20.9 vol%), c_i is the initial concentration of O_2 (vol%), L is the thickness of the unsaturated zone (m), D* is the effective diffusion coefficient for O_2 ($m^2 \cdot d^{-1}$), θ_a is the volumetric soil-air content, ρ_b is the dry bulk density ($g(\text{dry weight}) \cdot m^3$), G* is the O_2 consumption rate ($\mu g\ O_2 \cdot g(\text{dry weight})^{-1} \cdot d^{-1}$), and z is depth from ground surface (m). The D* values were calculated by the method of Fuller et al. (1966) and Millington and Quirk (1961):

$$D^* = \frac{\theta_a^{7/3}}{\theta^2} D \tag{3}$$

where θ is the porosity and D is the free-air diffusion coefficient (1.54 $m^2 \cdot d^{-1}$ at 20°C).

The O_2 consumption rates in Eqn. 1 were described by a function similar to that used by Hendry et al. (1999):

$$G^* = G_o \theta_a^2 \theta_w^2, \tag{4}$$

where G_o is a proportionality constant ($\mu g\ O_2 \cdot g(\text{dry weight})^{-1} \cdot d^{-1}$), and the volumetric soil-moisture content (θ_w) and θ_a represent the dependence of O_2 consumption on water content. At low θ_w, oxygen consumption decreases because of a lack of water; at high θ_w, aerobic microbial activity also decreases because of saturation of the pore spaces.

The Levenberg-Marquardt fitting routine (see Press et al., 1989) was used to fit the numerical solution of Eqn. 1 to the measured O_2 concentrations to determine the G_o value that resulted in the best fit between the modeled and measured O_2 data.

The numerical model was also verified against an independent analytical solution for Eqn. 1 under constant moisture content conditions and uniform O_2 consumption with depth through the unsaturated zone. The analytical solution used was (Papendick and Runkles, 1965)

$$C_{(z,\infty)} = C_o - \frac{G^*}{\theta_a D^*}\left(Lz - \frac{z^2}{2}\right). \tag{5}$$

After simulating the consumption and transport of the O_2, each of the isotopes ($^{16}O_2$ and $^{18}O^{16}O$) was addressed individually, whereby c in Eqn. 1 represented the concentration of either $^{16}O_2$, represented by $[^{16}O]$, or $^{18}O^{16}O$, represented by $[^{18}O]$. The measured concentration profiles of $[^{16}O]$ and $[^{18}O]$ were determined from

$$\delta^{18}O = \left(\frac{R_s}{R_{std}} - 1\right) 1000 \tag{6}$$

and

$$[^{16}O] + [^{18}O] = O_2 \tag{7}$$

where R_s is $[^{18}O]/[^{16}O]$ and R_{std} is 2.01×10^{-3}.

In modeling the consumption and transport of each isotope with Eqn. 1, the values of D and G* differ from that above and are defined below. In the case of D, the values are related by the isotope fractionation factor for diffusion (α_D) by

$$\alpha_D = {}^{18}D/{}^{16}D, \tag{8}$$

where ^{18}D is the diffusion coefficient for $^{18}O^{16}O$ and ^{16}D is the diffusion coefficient for $^{16}O_2$. In Eqn. 8, α_D in air is 0.986, as determined by Graham's Law (Clark and Fritz, 1997). Because ^{16}O is the dominant isotope in O_2 (i.e., 99.76%), we assumed that ^{16}D was the same as that for O_2. The ^{18}D was then determined by Eqn. 8, knowing ^{16}D and α_D.

In the case of $^{16}O_2$,

$$G^* = {}^{16}k[^{16}O], \tag{9}$$

and for $^{18}O^{16}O$,

$$G^* = {}^{18}k[^{18}O], \tag{10}$$

where ^{16}k and ^{18}k (hr^{-1}) represent the specific consumption rates for $^{16}O_2$ and $^{18}O^{16}O$ (Aggarwal and Dillon, 1998). The ^{16}k and ^{18}k values were related through

$$\alpha_k = {}^{18}k/{}^{16}k, \tag{11}$$

where α_k is the isotope fractionation factor due to microbial consumption by respiration. From Eqns. 9 and 10, and simulated best-fit G*, and $[^{16}O]$ and $[^{18}O]$ values, ^{18}k and ^{16}k values were determined. The resulting best-fit concentration profiles for the two isotopes were recombined in Eqn. 6 to yield a best-fit modeled $\delta^{18}O$ (VSMOW) profile.

Numerical modeling was performed with a 3.2-m grid corresponding to the unsaturated zone thickness. A uniform element size of 0.1 m and time steps of 1-d for a time period of 2000 d (to ensure that the numerical model attained steady state) were used.

The numerical models of transport and consumption of $[^{16}O]$ and $[^{18}O]$ were verified by means of a solution developed for uniform moisture content distribution (and thus uniform O_2 consumption) with depth. This solution was developed by writing Eqn. 5 in terms of $[^{16}O]$ and $[^{18}O]$, whereby

$$[^{18}O] = [^{18}O]_{atm} - \frac{[^{18}O]^{18}k}{\theta_a^{18} D^*}\left(Lz - \frac{z^2}{2}\right) \tag{12}$$

and

$$[^{16}O] = [^{16}O]_{atm} - \frac{[^{16}O]^{16}k}{\theta_a^{16}D^*}\left(Lz - \frac{z^2}{2}\right). \quad (13)$$

Eqn. 12 was divided by Eqn. 13 and simplified to yield

$$\left(\frac{[^{18}O] - [^{18}O]_{atm}}{[^{16}O] - [^{16}O]_{atm}}\right)\frac{\alpha_D}{\alpha_k} = \left(\frac{[^{18}O]}{[^{16}O]}\right). \quad (14)$$

Assuming a uniform and constant α_k, the ratio $[^{18}O]/[^{16}O]$ in Eqn. 14 was determined by an iterative approach. The $[^{18}O]$ and $[^{16}O]$ on the left side of Eqn. 14 were determined by the assumed ratio of $[^{18}O]/[^{16}O]$ and Eqns. 6 and 7. The O_2 concentration profile with depth (required for Eqn. 7) was calculated by Eqn. 5 for a uniform O_2 consumption rate. The resulting α_k and $\delta^{18}O$-depth profiles matched the values determined by the numerical model.

3. RESULTS AND DISCUSSION

The mean steady-state moisture content depth profile in the mesocosm is presented in Figure 1a (dashed line) for the time period between day 2254 and 2602 (n = 10). Moisture contents ranged from ~0.04% at 0.6 m to 10 to 14% between 1 and 2.5 m. Below 2.5 m, the moisture content increased through the capillary fringe to the water table at 3.2 m depth. The standard deviation on the moisture content data set was less than 1%. Drainage from the mesocosm increased from 0.3 $L \cdot d^{-1}$ on day 406 to 1.0 $L \cdot d^{-1}$ on day 633 (Hendry et al., 2001). Subsequent drainage measurements remained near 1.0 $L \cdot d^{-1}$. The invariant water flux and moisture content measurements indicated that the flux of water through the unsaturated zone was at steady state during the study period. Because the outflow from the mesocosm was 23% of the water applied (Hendry et al., 2001), the loss of the majority of the water applied was attributed to evaporation from the surface of the mesocosm. During the study period, the temperature of the mesocosm was uniform, ranging between 18°C and 20°C.

The O_2 and CO_2 gas concentration data between day 2254 and 2604 is summarized in Table 1 and the O_2 gas concentrations are plotted in Fig. 1b. Oxygen gas concentrations decreased from atmospheric concentrations (20.9 vol%) at ground surface to 19.2 vol% at 2.61 m depth, whereas CO_2 concentrations showed a concomitant increase with depth. The low standard deviation in all gas composition and concentration data collected between day 2254 and 2604 (Table 1) confirmed near-steady-state conditions existed in the mesocosm. The results of these gas analyses were consistent with those reported by Hendry et al. (2001) from day 350 to 840. The timing of gas sampling (i.e., before or after the application of water) had no measurable effect on the measured gas concentrations (Kabwe, 2001).

Three lines of evidence showed that O_2 consumption and CO_2 production in the mesocosm resulted from microbial respiration. First, microbial heterotrophs are present throughout the entire unsaturated zone of the mesocosm (Hendry et al., 2001). Second, $\delta^{13}C$-CO_2 measurements from the mesocosm show that biogenic CO_2 is derived from soil organic carbon present in the mesocosm ($\delta^{13}C = -21.0$ to -23.6‰; n = 26) (Strauch et al., 1996). Finally, the sum of CO_2 and O_2 gas concentrations yielded a mean value of 21.2 vol%, suggesting that ~1 mol of CO_2 gas was produced for each mole of O_2 gas consumed, again in keeping with microbial respiration. This suggested that the consumption of O_2 and oxidation of organic carbon can be approximated by the simplified oxidation-reduction reaction (Stumm and Morgan, 1981):

$$CH_2O + O_2 = CO_2 + H_2O, \quad (15)$$

where CH_2O represents sedimentary organic carbon as a simple carbohydrate.

The simulated O_2 concentration profile using measured moisture content data (Fig. 1a) (and assuming that moisture content at depths < 0.6 m was the same as at 0.6 m) is presented in Figure 1b (dashed line). It yielded a poor approximation to the measured O_2 concentration profile. The simulated profile produced lower O_2 concentrations than were measured throughout the upper 1.75 m of the mesocosm.

In contrast to the above simulation, the assumption of constant moisture content with depth (and therefore constant O_2 microbial consumption rate with depth) yielded an excellent fit to the measured O_2 data (Fig. 1b). In this case, moisture content was assumed to be equal to the mean moisture content of the sand (~13%; Fig. 1a) measured between the depths of 0.64 and 3.19 m. The use of the mean moisture content was a reasonable assumption that was based on the uniform grain-size distribution of the sand. Furthermore, the use of a simplified model for O_2 consumption by respiration was considered reasonable in this case because the unsaturated zone consisted solely of homogenized C-horizon sand and contained no plant or soil organic horizons. Papendick and Runkles (1965) also applied the use of a constant respiration rate with depth for O_2 consumption.

The results of the O_2 consumption and transport modeling yielded similar rates and fluxes to the biogenic CO_2 production and transport modeling done by Hendry et al. (2001) on the same mesocosm, although the fluxes were in opposite directions. For example, the modeled O_2 consumption rates that used the mean and constant moisture content profiles typically ranged from 0.2 to 0.7 $\mu g\ O_2 \cdot g\ soil^{-1} \cdot d^{-1}$ (Fig. 1c). These O_2 consumption rates were in keeping with uniform biogenic CO_2 production rates calculated for the mesocosm between day 495 to 837 (0.2 $\mu g\ C \cdot g^{-1} \cdot d^{-1}$). These respiration rates are two to three orders of magnitude greater than those reported for a corresponding, undisturbed field site (Hendry et al., 1999). In addition, calculated surface fluxes of O_2 in the current study were 62 and 49 mmol $O_2 \cdot m^2 \cdot d$ for the mean and constant moisture content models. These fluxes were similar to estimated CO_2 surface fluxes from the mesocosm from day 495 to 837 (59 mmol $CO_2 \cdot m^2 \cdot d$). The similarity in these results suggested that the numerical model used in the current study yielded consistent results to that presented in Hendry et al. (2001) for biogenic CO_2 production and redistribution.

Additional O_2 simulations showed that, as expected, the fit between modeled and measured O_2 concentration depth profiles did not change with variations in the assumed uniform moisture content. Varying the assumed moisture content did, however, change the calculated flux of O_2. The calculated O_2 fluxes ranged from 37 to 120 mmol $O_2 \cdot m^2 \cdot d$ for constant moisture contents ranging from 15 to 3%, respectively.

Keller and Bacon (1998) suggest that enhanced microbial activity occurs near the capillary surface, just above the water table. The effect of enhanced microbial activity at the capillary fringe on the concentration profiles of O_2 was investigated by

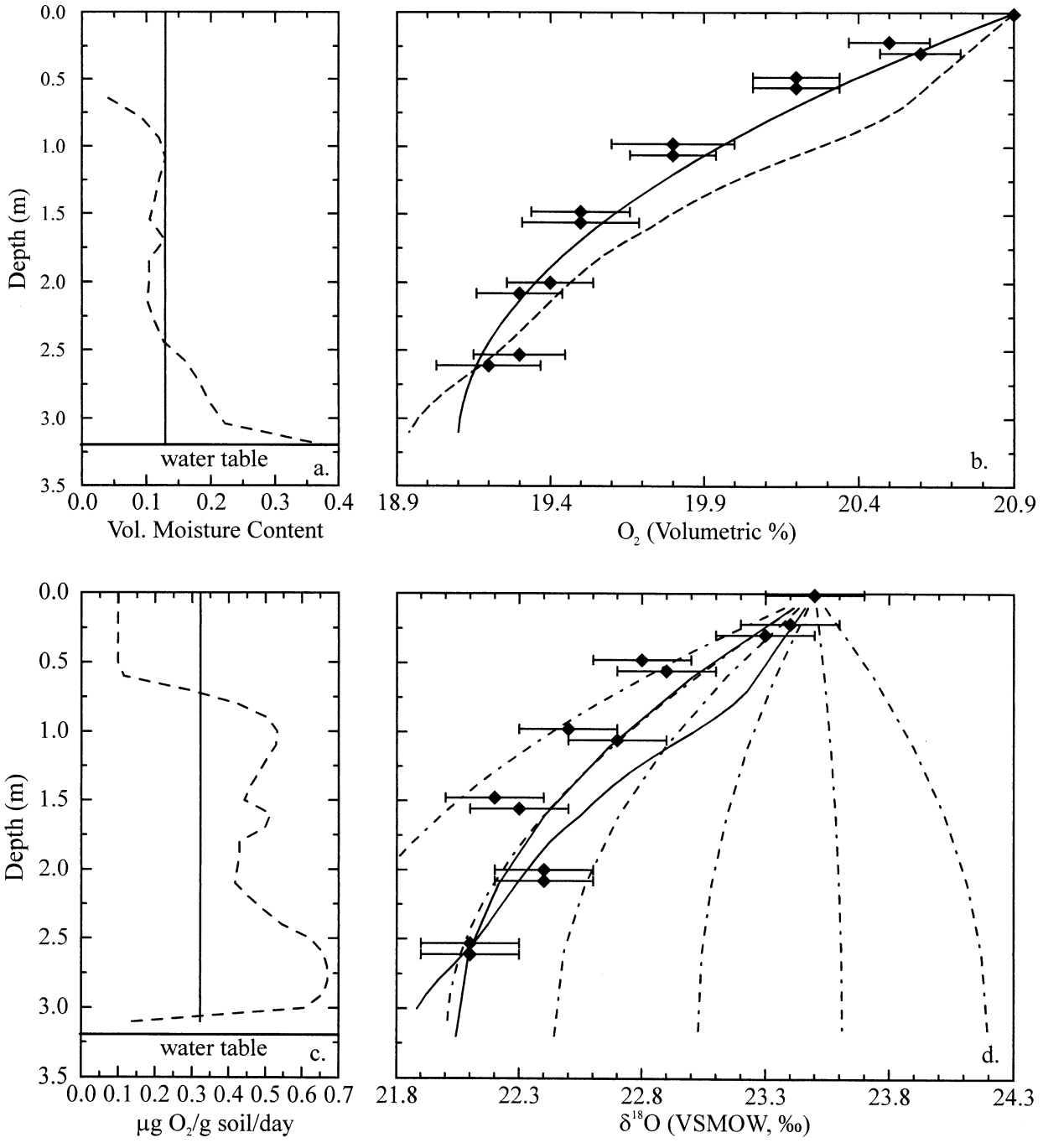

Fig. 1. Distribution of (a) moisture content, (b) O_2 gas concentrations, (c) microbial consumption rates, and (d) $\delta^{18}O$ of O_2 through the unsaturated zone in the mesocosm. The dashed line and solid line in (a) represent the mean measured moisture content profile from day 2254 to 2602 and an assumed constant moisture content profile, respectively. The data points and the horizontal bars in (b) represent the mean measured O_2 concentrations and standard deviations, respectively, from both the west and east nest of samplers. The data points and horizontal bars in (d) represent the mean $\delta^{18}O$ values and analytical precision, respectively, for both the west and east nest of samplers. Best-fit results of simulated diffusive transport and consumption of O_2 and its isotopes for the mean measured moisture content conditions and assumed constant moisture content conditions are presented in (b), (c), and (d) as dashed and solid lines, respectively. The irregularly dashed lines in (d) represent the theoretical distribution of $\delta^{18}O$ of O_2 under a constant O_2 consumption rate for a range in α_k values from 1.005, 1.000 (diffusion only), 0.995, 0.991, 0.985, and 0.980 (from left to right on figure).

Table 1. CO_2, O_2, and $\delta^{18}O$ analyses of gas samples collected from the unsaturated mesocosm.[a]

Depth (m)	CO_2 (vol%)	O_2 (vol%)	$\delta^{18}O$ (‰, VSMOW)
Air	0.036	20.95	+23.5 ± 0.2 (5)
East nest			
0.22	0.36 ± 0.01 (37)	20.5 ± 0.13 (37)	+23.4 ± 0.2 (2)
0.48	0.88 ± 0.04 (37)	20.2 ± 0.14 (37)	+22.8 ± 0.1 (2)
0.98	1.41 ± 0.06 (37)	19.8 ± 0.20 (37)	+22.5 (1)
1.48	1.71 ± 0.09 (37)	19.5 ± 0.16 (37)	+22.2 (1)
2.00	1.82 ± 0.09 (37)	19.4 ± 0.14 (37)	+22.4 ± 0.3 (2)
2.53	1.87 ± 0.09 (37)	19.3 ± 0.15 (37)	+22.1 (1)
West nest			
0.30	0.39 ± 0.02 (37)	20.6 ± 0.13 (37)	+23.3 ± 0.2 (3)
0.56	0.88 ± 0.04 (37)	20.2 ± 0.14 (37)	+22.9 ± 0.1 (2)
1.06	1.43 ± 0.07 (37)	19.8 ± 0.14 (37)	+22.7 ± 0.1 (4)
1.56	1.82 ± 0.09 (37)	19.5 ± 0.19 (37)	+22.3 ± 0.1 (3)
2.08	1.94 ± 0.10 (37)	19.3 ± 0.14 (37)	+22.4 ± 0.1 (4)
2.61	1.98 ± 0.12 (37)	19.2 ± 0.17 (37)	+22.1 (1)

Data are expressed as mean ± standard deviation (number of analyses).

conducting additional simulations. In these simulations, O_2 consumption was restricted to a depth interval of 3.0 to 3.2 m. The simulations showed that the distribution of O_2 poorly approximated the measured data set under these assumptions; the simulated O_2 profiles yielded straight-line relationships extending from the lower values in the active zone (the capillary fringe) to atmospheric conditions at ground surface. Thus, these results clearly showed that microbial activity could not be solely focused at the capillary fringe in the mesocosm. Similar results were found by Hendry et al. (2001) for microbial respiration rates in the mesocosm, a finding based on CO_2 analyses.

The results of $\delta^{18}O$ analyses of O_2 are presented in Table 1 and Figure 1d. The $\delta^{18}O$ values decreased with depth from an atmospheric value of +23.5‰ (VSMOW) at ground surface to +22.1‰ at 2.61 m depth. These data revealed an overall negative oxygen isotope shift of −1.4‰. Severinghaus et al. (1996) measured a negative isotopic shift in $\delta^{18}O$ of O_2 gas collected to depths of up to 70 m in a California desert sand dune. The maximum isotopic shift there was less than −0.4‰, and was attributed to oxygen isotopic fractionation due to upward water vapor flux from the water table to the atmosphere. This fractionation process observed by Severinghaus et al. (1996) was not expected in this study. The soil in the mesocosm was moist below depths of 0.75 m, and therefore, a gradient in relative humidity would not exist. Aggarwal and Dillon (1998) measured the $\delta^{18}O$ of O_2 in soil gas at a site in Nebraska. At this site, soil gas samples were collected from five monitoring wells installed at depths between 3 to 4 m in a 6-m thick unsaturated zone consisting of silty clay and sand. In contrast to our results and the results of Severinghaus et al. (1996), the $\delta^{18}O$ values observed by Aggarwal and Dillon (1998) at the Nebraska site were significantly more positive than the atmospheric isotopic value of O_2, and ranged from +24.0‰ to +27.2‰. Aggarwal and Dillon (1998) also measured $\delta^{18}O$ values ranging from +21.2 to +22.9‰ at a site in Texas. These lower $\delta^{18}O$ values were attributed to less consumptive fractionation.

The best-fit simulated $\delta^{18}O$ profiles from the two moisture content conditions (Fig. 1a) are presented in Figure 1d. As with O_2 concentrations, the best fit for $\delta^{18}O$ was obtained by using a simplified assumption of constant moisture content conditions with depth. In both simulations, however, the best-fit α_k value was determined to be exactly 1.00 (Fig. 1d). This suggested that there was little or no oxygen isotopic fractionation due to microbial respiration in the mesocosm. Unfortunately, our inability to measure O_2 in soil gas concentrations beyond three significant figures resulted in a corresponding α_k value of only three significant figures. Because α_k values for microbial respiration reported in the literature are typically presented using four significant figures, the calculated α_k values in the mesocosm could in fact be 1.000 ± 0.005.

The measured O_2 concentrations were plotted vs. the $\delta^{18}O$ values (Fig. 2) to obtain a more accurate estimate of α_k values in the mesocosm. A straight line originating at atmospheric values yielded the equation

$$\delta^{18}O = 0.815O_2 + 6.464. \quad (16)$$

Eqn. 16 provided a good fit to the measured data ($r^2 = 0.92$). Results of the analytical solutions that were based on a uniform moisture content of 13% over a range in α_k values also yielded straight-line relationships between O_2 concentrations and $\delta^{18}O$ values (Fig. 2). Comparing plots of these simulated data sets to our measured data confirmed that an α_k value of 1.000 (no isotopic fractionation) likely best represented microbial activity in the mesocosm. This modeled α_k value was somewhat higher than the range of α_k values reported for microbial respiration in the literature. Most laboratory microbial respiration experiments yielded α_k values between 0.971 to 0.999 (Lane and Dole, 1956; Schleser, 1978, 1979; Guy et al., 1989, 1993; Bender, 1990; Kiddon et al., 1993; Aggarwal and Dillon, 1998; Revesz et al., 1999; Angert et al., 2001). Had the α_k in the mesocosm been similar to values of microbial respiration reported in this literature (e.g., $\alpha_k = 0.982$), the resulting $\delta^{18}O$-depth profile would instead be considerably shifted to the right in Figure 1d, and upward in Figure 2. Bender et al. (1994) and Angert and Luz (2001) reported that oxygen isotope discrimi-

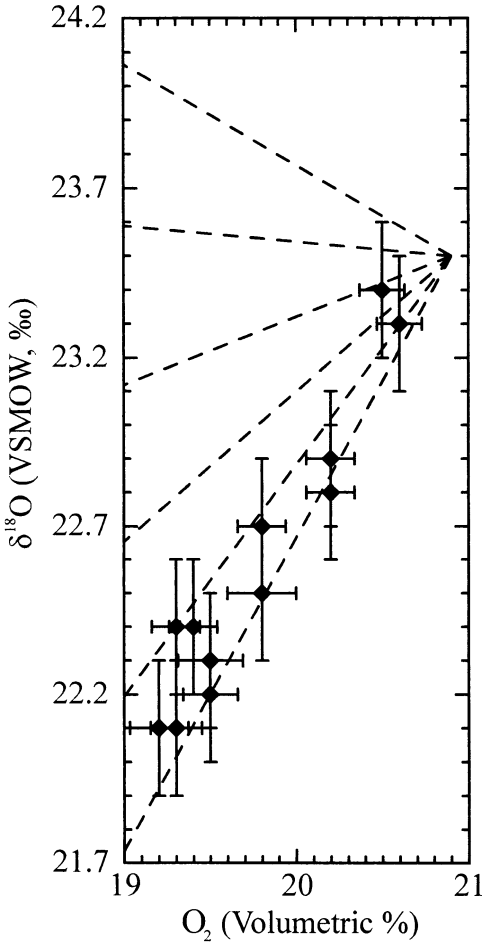

Fig. 2. Mean oxygen concentrations vs. associated $\delta^{18}O$ values of the O_2 collected from gas samples in the unsaturated zone of the mesocosm. Vertical bars represent the precision of the $\delta^{18}O$ measurements, and horizontal bars represent the standard deviation of the O_2 concentration measurements. Best-fit results of simulated diffusive transport and consumption of O_2 and its isotopes under assumed constant moisture content conditions are presented for a range in α_k values as dashed lines. The lines represent α_k values of 1.005, 1.000 (diffusion only), 0.995, 0.990, 0.985, and 0.980 (from bottom to top in figure).

nation in partially closed systems depends on both biochemical mechanisms and gaseous diffusion. In cases where O_2 concentrations are limited, the overall α_k is expected to approach 1.000. In this case, microorganisms with high activity rates and located in microenvironments that are resistant to O_2 diffusion may not discriminate between isotopomers of O_2. Indeed, the measured microbial respiration rates in the mesocosm were two to three orders of magnitude greater than the associated in situ field rates (Hendry et al., 2001). Resistance to oxygen diffusion could be provided if the fine sand in the mesocosm formed soil aggregates during drying after placement or possibly by the presence of a water film around microbial microenvironments.

In conclusion, we have demonstrated an oxygen isotope tracer and modeling approach that may aid in gaining a better understanding of biogenic gas production and O_2 cycling in subsurface systems and soils. Although the highly controlled, steady-state mescosom findings reported here may not be directly transferable to natural field settings, the tracer and modeling approach can be applied to field-based experiments. Additionally, the isotope tracer and transport modeling technique can also be used in conjunction with measured O_2 concentrations and the numerical model to estimate in situ oxygen isotope fractionation factors. In this controlled mesocosm study, we found that at very high respiration rates there appeared to be very little isotope fractionation of O_2 by microorganisms. Although the high microbial respiration rates we observed in the mesocosm are obviously not typical of natural soils in northern temperate climes, they may in fact be more representative of soil conditions found in warm and moist tropical environments. Hendry et al. (2001) reported that C-horizon respiration rates in the mesocosm used in this study were among the highest reported in the literature and similar to that of a C-horizon in a forested site in the Amazon (Davidson and Trumbore, 1995; Selker et al., 1999). Our findings also caution against the indiscriminate use of laboratory-determined oxygen isotope fractionation factors to field settings. Finally, microbial respiration is a primary and important factor that controls the chemistry and isotopic characteristics of recharging groundwater; thus, field-based studies of oxygen cycling are needed at a variety of field sites with more complex but naturally representative unsaturated zones. These unsaturated profiles should contain natural organic soil zones and transient thermal, moisture content, and gas profiles.

Acknowledgments—Funding for this work was provided by research grants from the Natural Science and Engineering Research Council of Canada (M.J.H.) and from the National Water Research Institute, Environment Canada (L.I.W.). Louis Kabwe measured gas concentrations and moisture contents in the mesocosm during the study period, and Geoff Koehler assisted with the oxygen isotopic analyses. We gratefully acknowledge the support provided by Carl Mendoza, University of Alberta, Canada, with the development of the finite-element model.

Associate editor: N. E. Ostrom

REFERENCES

Aggarwal P. K., Fuller M. E., Gurgas M. M., Manning J. F., and Dillon M. A. (1997) Use of stable oxygen and carbon isotope analyses for monitoring the pathways and rates of intrinsic and enhanced in situ biodegradation. *Environ. Sci. Technol.* **31,** 590–696.

Aggarwal P. and Dillon M. A. (1998) Stable isotopic composition of molecular oxygen in soil gas and groundwater: A potentially robust tracer for diffusion and oxygen consumption processes. *Geochim. Cosmochim. Acta* **62,** 577–584.

Angert A. and Luz B. (2001) Fractionation of oxygen isotopes by root respiration: Implications for the isotopic composition of atmospheric O_2. *Geochim. Cosmochim. Acta* **65,** 1695–1701.

Angert A., Luz B., and Yakir D. (2001) Fractionation of oxygen isotopes by respiration and diffusion in soils and its implications for the isotopic composition of atmospheric O_2. *Global Biogeochemical Cycles* **15**(4), 871–880.

Bender M. L. (1990) The $\delta^{18}O$ of dissolved O_2 in seawater: A unique tracer of circulation and respiration in deep sea. *J. Geophys. Res.* **95,** 22243–22252.

Bender M., Sowers T., and Labeyrie L. (1994) The Dole effect and its variations during the last 130,000 years as measured in the Vostok ice core. *Global Biogeochem. Cycles* **8,** 363–376.

Blake D. R. and Rowland F. S. (1988) Continuing worldwide increase in tropospheric methane, 1978 to 1987. *Science* **239,** 1129–1131.

Chapelle F. H. (1992) *Ground-Water Microbiology and Geochemistry*. Wiley.

Clark I. D. and Fritz P. (1997) *Environmental Isotopes in Hydrogeology*. Lewis Publishers.

Davidson E. A. and Trumbore S. E. (1995) Gas diffusivity and production of CO_2 in deep soils of the eastern Amazon. *Tellus* **47B,** 550–565.

Fuller E. N., Schettler P. D., and Giddings J. C. (1966) A new method for prediction of binary gas-phase diffusion coefficients. *Ind. Eng. Chem.* **58,** 19–27.

Guy R. D., Berry J. A., Fogel M. L., and Hoering T. C. (1989) Differential fractionation of oxygen isotopes by cyanide-resistant and cyanide-sensitive respiration in plants. *Planta* **177,** 483–491.

Guy R. D., Fogel M. L., and Berry J. A. (1993) Photosynthetic fractionation of the stable isotopes of oxygen and carbon. *Plant Physiol.* **101,** 37–47.

Hall A. J., Connor D. J., and Whitfield D. M. (1990) Root respiration during grain filling in sunflower: The effects of water stress. *Plant Soil* **121,** 57–66.

Hendry M. J., Mendoza C. A., Kirkland R., and Lawrence J. R. (1999) Quantification of transient CO_2 production. *Water Resources Res.* **35,** 2189–2198.

Hendry M. J., Mendoza C. A., Kirkland R., and Lawrence J. R. (2001) An assessment of a mesocosm approach to the study of microbial respiration in a sandy unsaturated zone. *Ground Water* **39,** 391–400.

Hoefs J. (1987) *Stable Isotope Geochemistry*. Springer-Verlag.

Kabwe L. K. (2001) Design and application of a dynamic closed chamber system for measuring CO_2 fluxes from unsaturated C-horizon soils and waste-rock piles to the atmosphere. M.Sc. thesis. University of Saskatchewan, Canada.

Kabwe L. K., Hendry M. J., Wilson G. M., and Kirkland R. A. (2002) Quantification of CO_2 fluxes from the surface of a minicosm to the atmosphere. *J. Hydrol.* **260**(1/4), 1–14.

Keller C. K. and Bacon D. H. (1998) Soil respiration and georespiration distinguished by transport analyses of vadoze CO_2, $^{13}CO_2$, and $^{14}CO_2$. *Global Biogeochem. Cycles* **12,** 361–372.

Kiddon J., Bender M. L., Orchardo J., Caron D. A., Goldman J. C., and Dennett M. (1993) Isotopic fractionation of oxygen by respiring marine organisms. *Global Biogeochem. Cycles* **7,** 679–694.

Kroopnick P. and Craig H. (1972) Atmospheric oxygen: Isotopic composition and solubility fractionation. *Science* **175,** 54–55.

Lane G. A. and Dole M. (1956) Fractionation of oxygen isotopes during respiration. *Science* **123,** 574–576.

Langmuir D. (1997) *Aqueous Environmental Geochemistry*. Prentice-Hall.

Lawrence J. R., Zanyk B. N., Wolfaardt G. M., Hendry M. J., Robarts R. D., and Caldwell D. E. (1993) Design and evaluation of a mesoscale model vadose zone and ground water system. *Ground Water* **31,** 446–455.

Matson P. A. and Harris R. C. (1995) *Biogenic Trace Gases: Measuring Emissions from Soil and Water*. Blackwell Scientific.

Millington J. R. and Quirk J. P. (1961) Permeability of porous solids. *Trans. Faraday Soc.* **57,** 1200–1207.

Neale C. N., Hughes J. B., and Ward C. H. (2000) Impacts of unsaturated zone properties on oxygen transport and aquifer reaeration. *Ground Water* **35,** 784–794.

Norman J. N., Garcia R., and Verma S. B. (1992) Fluxes and carbon budget of grassland. *J. Geophys. Res.* **97,** 18845–18853.

Papendick R. I. and Runkles J. R. (1965) Transient-state oxygen diffusion in soil: I. The case when rate of oxygen consumption is constant. *Soil Sci.* **100,** 251–261.

Press W. H., Flannery B. P., Teukolsky S. A., and Vetterling W. T. (1989) *Numerical Recipes (FORTRAN Version)*. Cambridge University Press.

Revesz K., Coplen T. B., Baedecker M. J., Glynn P. D., and Hult M. (1995) Methane production and consumption monitored by stable H and C isotope ratios at a crude oil spill site, Bemidji, Minnesota. *Appl. Geochem.* **10,** 505–516.

Revesz K., Bohlke J. K., Smith R. L., Yoshinari T. (1999) $\delta^{18}O$ composition of dissolved O_2 undergoing respiration in a contaminated ground water: IAEA International Symposium on Isotope Techniques in Water Resources Development and Management, Vienna, Austria, 10–14 May 1999, International Atomic Energy Agency, Vienna, CD-ROM.

Rochette P., Desjardins R. L., and Pattey E. (1991) Spatial and temporal variability of soil respiration in agricultural fields. *Can. J. Soil Sci.* **10,** 189–196.

Rose S. and Long A. (1988) Dissolved oxygen systematics in the Tuscon Basin aquifer. *Water Resources Res.* **24,** 127–136.

Schleser G. H. (1978) Contribution of the respiratory oxygen isotope fractionation to the ^{18}O budget of the atmosphere. *Environmental Biogeochemistry and Geomicrobiology*, (ed. W. E. Krumbein), pp. 825–835. Ann Arbor Scientific Publishing.

Schleser G. H. (1979) Oxygen isotope fractionation during respiration for different temperatures of. *T. utilis* **17,** 85–93.

Selker J. S., Keller C. K., and McCord J. T. (1999) *Vadose Zone Processes*. Lewis Publishers.

Severinghaus J. P., Bender M. L., Keeling R. F., and Broecker W. S. (1996) Fractionation of soil gases by diffusion of water vapor, gravitational settling, and thermal diffusion. *Geochim. Cosmochim. Acta* **60,** 1005–1018.

Solomon D. K. and Cerling T. E. (1987) The annual carbon dioxide cycle in a montaine soil: Observations, modeling, and implications for weathering. *Water Resources Res.* **23,** 2257–2265.

Strauch G., Hendry M. J., Kirkland R., Wassenaar L. I., and Lawrence J. R. (1998) An isotopic study of microbial activity in vadose zone: A field and mesocosm laboratory study. In: Isotopic techniques in the study of Environmental Change. Proceedings of the International Atomic Energy Agency, International Atomic Energy Agency, Vienna.

Striegl R. G. and Wickland K. P. (1998) Effects of clear-cut harvest on soil respiration in a jack pine-lichen woodland. *Can. J. Forest Res.* **28,** 535–539.

Stumm W. and Morgan J. J. (1981) *Aquatic Chemistry*. Wiley-Interscience.

Taylor B. E., Wheeler M. C., and Nordstrom D. K. (1984) Stable isotope geochemistry of acid mine drainage: Experimental oxidation of pyrite. *Geochim. Cosmochim. Acta* **48,** 2669–2684.

Trumbore S. E., Chadwick O. A., and Amundson R. (1996) Rapid exchange between soil carbon and atmospheric carbon dioxide driven by temperature change. *Science* **272,** 393–396.

Wassenaar L. I. and Koehler G. (1999) An on-line technique for the determination of the $\delta^{18}O$ and $\delta^{17}O$ of gaseous and dissolved oxygen. *Anal. Chem.* **71,** 4965–4968.

Wood W. W. and Petraitis M. J. (1984) Origin and distribution of carbon dioxide in the unsaturated zone of the southern high plains of Texas. *Water Resources Res.* **20,** 1193–1208.

Wood D. B., Keller C. K., and Johnstone D. L. (1993) In situ measurements of microbial activity and controls on microbial CO_2 production in the unsaturated zone. *Water Resources Res.* **29,** 647–659.